Research Square

Preprints are preliminary reports that have not undergone peer review.
They should not be considered conclusive, used to inform clinical practice,
or referenced by the media as validated information.

Establishment and characterization of two gemcitabine-resistant cholangiocarcinoma cell lines

Haidong Ma
Lanzhou University First Clinical Medical College: Lanzhou University First Hospital
Jintao Li
Lanzhou University First Clinical Medical College: Lanzhou University First Hospital
Zhili Xia
Lanzhou University First Clinical Medical College: Lanzhou University First Hospital
Jiahui Xi
Lanzhou University First Clinical Medical College: Lanzhou University First Hospital
Zihe Dong
Lanzhou University First Clinical Medical College: Lanzhou University First Hospital
Wenan Wang
Lanzhou University First Clinical Medical College: Lanzhou University First Hospital
Ruyang Zhong
Lanzhou University First Clinical Medical College: Lanzhou University First Hospital
Yanyan Lin
Lanzhou University First Clinical Medical College: Lanzhou University First Hospital
Leiqing Wang
Lanzhou University First Clinical Medical College: Lanzhou University First Hospital
Kecheng Jin
Lanzhou University First Clinical Medical College: Lanzhou University First Hospital
Chongfei Huang
Lanzhou University First Clinical Medical College: Lanzhou University First Hospital
Liang Tian
Lanzhou University First Clinical Medical College: Lanzhou University First Hospital
Jinyu Zhao
Lanzhou University First Clinical Medical College: Lanzhou University First Hospital
Ningzu Jiang
Lanzhou University First Clinical Medical College: Lanzhou University First Hospital
Yawen Lu
Lanzhou University First Clinical Medical College: Lanzhou University First Hospital
Yeying Wang

Lanzhou University First Clinical Medical College: Lanzhou University First Hospital

Long Gao

Lanzhou University First Hospital

Wenbo Meng

mengwb@lzu.edu.cn

Lanzhou University First Affiliated Hospital: Lanzhou University First Hospital

---

Research Article

Keywords: cholangiocarcinoma, cell line, gemcitabine, drug resistance, transcriptome sequencing

Posted Date: September 12th, 2026

DOI: https://doi.org/10.21203/rs.3.rs-10833620/v1

License: This work is licensed under a Creative Commons Attribution 4.0 International License.
Read Full License

Establishment and characterization of two gemcitabine-resistant cholangiocarcinoma cell lines

Abstract

Cholangiocarcinoma (CCA) features high malignancy, concealed early symptoms and poor overall survival. Gemcitabine (GEM) plus cisplatin in combination with immune checkpoint inhibitors is a first-line chemotherapy regimen for advanced biliary tract cancer, yet acquired drug resistance severely restricts therapeutic efficacy. Available gemcitabine-resistant cholangiocarcinoma cell lines are relatively limited, and additional drug-resistant cell models should be established to supply adequate experimental materials for exploring cholangiocarcinoma gemcitabine-resistance mechanisms. This study aimed to construct stable high-resistance GEM-resistant CCA sublines derived from intrahepatic HuCCT-1 and extrahepatic TFK-1 parental cells and characterize their phenotypic and molecular features. Long-term dose-escalation GEM induction lasting 12–18 months was applied to build resistant sublines. HuCCT-1-GEM-2 (RI=24.8) and TFK-1-GEM-2 (RI=14.4) with stable high resistance were successfully established. Both drug-resistant cell lines exhibited increased cell volume, irregular morphology, accumulation of intracellular vacuoles, mitochondrial damage, and reduced proliferation rates, and developed selective cross-resistance to 5-FU. Transcriptome sequencing combined with qRT-PCR validation showed that key molecules of the NF-κB/inflammatory pathway were significantly altered in the HuCCT-1-GEM-2 resistant line, whereas the differentially expressed molecules in the TFK-1-GEM-2 resistant line were mainly enriched in the complement pathway and the sphingolipid metabolism pathway. Key molecules of the glycolysis pathway and the TNF/IL-17 signaling pathway showed significant expression changes in both resistant subtypes. The above results indicate that intrahepatic and extrahepatic cholangiocarcinoma may activate different core regulatory pathways during the development of drug resistance, while metabolic reprogramming and remodeling of inflammatory responses may represent adaptive changes shared by both.

Keywords: cholangiocarcinoma; cell line; gemcitabine; drug resistance; transcriptome sequencing

Introduction

Cholangiocarcinoma (CCA) is a highly heterogeneous malignant tumor originating from the biliary epithelium and is classified into intrahepatic and extrahepatic subtypes based on anatomical location[1, 2]. Its global incidence and mortality rates have increased continuously in recent decades. Owing to insidious early symptoms and rapid progression, over 80% of patients are diagnosed at locally advanced or metastatic stages and cannot undergo radical surgery, resulting in an extremely poor clinical prognosis with an overall 5-year survival rate of less than 10%[3, 4]. Gemcitabine is a core first-line chemotherapeutic agent for advanced CCA. Nevertheless, universal chemoresistance has emerged as the primary driver of treatment failure and tumor progression[5]. Clinical follow-up data have demonstrated that the median progression-free survival of patients receiving GEM-based regimens is merely 8.0 months, with long-term survival rates below 5%. Although accumulating evidence has revealed GEM resistance in CCA, distinct anatomical origins and cellular backgrounds give rise to divergent resistance phenotypes and molecular pathways, the heterogeneous mechanisms of which remain insufficiently elucidated[6-8].

In vitro cell models are vital tools for identifying tumor chemoresistance mechanisms. Most reported GEM-resistant CCA cell lines were established through short-term drug exposure, yielding low RI (mostly 2–5-fold) that fail to recapitulate acquired resistance following prolonged clinical treatment. Moreover, the majority of relevant studies have only employed a single cell line, making it not feasible to distinguish between universal and cell-specific resistance pathways[9]. In addition, certain intrinsic drug-tolerant CCA cell lines have rarely been characterized, which limits the discovery of resistance mechanisms and the development of targeted therapeutics.

To address these limitations, two complementary parental CCA cell lines were

selected in this study: HuCCT-1 (intrinsically GEM-resistant intrahepatic CCA) and TFK-1 (extrahepatic CCA)[10, 11]. Two stable acquired GEM-resistant sublines, HuCCT-1-GEM-2 and TFK-1-GEM-2, were successfully established through a long-term dose-escalation induction protocol lasting 12–18 months, yielding RIs of 24.8 and 14.4, respectively, exceeding those achieved with conventional short-term induction models. Multiple assays, including cellular morphological observation, ultrastructural analysis, proliferation detection, high-throughput transcriptome sequencing, and qRT-PCR validation, were integrated to comprehensively characterize resistant cellular phenotypes and screen for differentially expressed genes (DEGs) and core signaling pathways.

The high-RI dual- cell models constructed in this study more closely recapitulated the clinical resistance status. By comparing the molecular signatures of intrahepatic- and extrahepatic-resistant CCA cells, we systematically investigated the conserved and subtype-specific regulatory networks potentially involved in GEM resistance. These findings expand the current understanding of CCA chemoresistance and provide experimental evidence and candidate therapeutic targets for strategies to overcome drug resistance and develop combination therapies.

Materials and Methods

1. Cell Culture

Human intrahepatic cholangiocarcinoma cell lines HuCCT-1, RBE and HCCC-9810 were purchased from the Cell Bank of Type Culture Collection of the Chinese Academy of Sciences (Shanghai, China). The human extrahepatic cholangiocarcinoma cell line TFK-1 was obtained from Abace Biotechnology. Human intrahepatic CCA HuCCT-1 and extrahepatic TFK-1 cells were cultured in RPMI 1640 medium supplemented with 10% fetal bovine serum (FBS, Cell-Box,AUS-01S-02) at 37 °C in a humidified incubator with 5% CO_2.

2. Establishment of HuCCT-1-GEM-2 and TFK-1-GEM-2 Resistant Cell Lines

The gemcitabine-resistant subline HuCCT-1-GEM-2 was induced from parental HuCCT-1 cells via a stepwise dose-escalation strategy. The initial gemcitabine

concentration was set at 2 μM, followed by a 2 μM incremental increase per induction cycle until the final concentration of 40 μM was reached, with the entire induction process lasting 18 months. Upon completion of drug induction, HuCCT-1-GEM-2 cells were cultured in drug-free complete medium for 2 months. Subsequently, HuCCT-1 and HuCCT-1-GEM-2 cells were exposed to a series of gemcitabine concentrations for 48 h, and the half-maximal inhibitory concentration (IC50) of gemcitabine for both cell lines was calculated.

For the TFK-1 cell line, its gemcitabine-resistant subline TFK-1-GEM-2 was also generated by stepwise gemcitabine dose escalation. Induction was initiated at 0.5 μM gemcitabine, with a concentration increment of 0.8 μM per cycle up to a maximum concentration of 10μM, and the whole induction period took 12 months. After drug withdrawal, TFK-1-GEM-2 cells were maintained in drug-free medium for 2 months. Afterwards, parental TFK-1 and resistant TFK-1-GEM-2 cells were treated with gradient gemcitabine concentrations for 48 h to determine their respective IC50 values. The gemcitabine-resistant human cholangiocarcinoma cell lines HuCCT-1-GEM-2 and TFK-1-GEM-2 have been deposited at the China Center for Type Culture Collection (CCTCC) under the accession numbers CCTCC NO: C2023103 and CCTCC NO: C2023104.

3. Cell Proliferation Assay

Logarithmically growing cells were seeded into 96-well plates with 100 μL single-cell suspension per well. After 12 h of incubation until cells formed a confluent monolayer at the bottom of each well, the original culture medium was discarded. CCK-8 solution(APEx BIO, K1018) was added at 0 h, 24 h, 48 h, 72 h and 96 h, followed by absorbance measurement at 450 nm to calculate cell proliferation rates. All experiments were repeated three times independently.

4. Transmission Electron Microscopy (TEM)

Two paired cell models were used in this study: HuCCT-1/HuCCT-1-GEM-2 and TFK-1/TFK-1-GEM-2. Cells reaching 90% confluence were digested with trypsin

and harvested by centrifugation. After resuspension in PBS and a second round of centrifugation, the supernatant was discarded, and cell pellets were fixed overnight in 2.5% glutaraldehyde at 4 °C. The fixed pellets were resuspended in 1 mL PBS and centrifuged, followed by shaking incubation for 15 min; this washing procedure was repeated three times. For embedding, 1.5% agarose was heated in a 90 °C water bath for 2 min, cooled to 45 °C, fully mixed with cell precipitates, and centrifuged at 3000 rpm for 2 min. The mixture was cooled at 4 °C for 10 min. Subsequently, ultra-thin frozen sections(Leica,EM UC7) were prepared, and images were captured under a transmission electron microscope(Thermo Fisher,200KVTalos F200C).

5. Quantitative Real-Time PCR (qRT-PCR)

Total cellular RNA was extracted using TRIzol reagent. RNA purity was detected with a micro-spectrophotometer, with OD260/280 values ranging from 1.8 to 2.1 and OD260/230 values greater than 1.9. A total of 1 μg qualified total RNA was used as the template for reverse transcription to synthesize cDNA. Quantitative real-time PCR (qRT-PCR) was performed using TB Green dye, with β-Actin serving as the internal reference gene. The amplification procedure was as follows: initial denaturation at 95 °C for 30 s, followed by 40 cycles of 95 °C for 5 s and 60 °C for 30 s. Melting curve analysis was carried out after amplification, and a single sharp melting peak was observed for all amplicons, verifying specific amplification. The 2^(−ΔΔCt) method was applied to calculate the relative gene expression levels, and three independent biological replicates were set for each group. Table 1 shows the primer sequences of target genes.

Table 1. Primer sequences for target genes

Gene Name	Forward Primer (5'→3')	Reverse Primer (5'→3')
β-Actin	AGAGGGAAATCGTGCGTGAC	CAATAGTGATGACCTGGCCGT
NFKB1	CACAAGGCAGCAAATAGACG	GAGTTAGCAGTGAGGCACCA
IL6	CAATAACCACCCCTGACCCA	TCTGAGGTGCCCATGCTACA
HK2	GAGCCACCACTCACCCTACT	CCAGGCATTCGGCAATGTG
PKM	ATGTCGAAGCCCCATAGTGAA	TGGGTGGTGAATCAATGTCCA
IL17A	CACCGCAATGAAGACCCTGA	TTCCCTCCGCATTGACACAG
TNF	GAGGCCAAGCCCTGGTATG	CGGGCCGATTGATCTCAGC
CAV1	AAGTACGACGCGCACACCAA	GATGTTGCCCTTGATGGTGAA
C3	GCTGGAGAAGTTCTGGGTGA	GGTGATGGTGATGGTGGTGT
SPHK1	GCTGGCAGCTTCCTTGAACCAT	GTGTGCAGAGACAGCAGGTTCA

6. High-Throughput Transcriptome Sequencing

Three biological replicates each of HuCCT-1, HuCCT-1-GEM-2, TFK-1 and TFK-1-GEM-2 cells were collected for total RNA extraction and quality assessment. mRNA was enriched, fragmented, and reverse-transcribed to synthesize first-strand cDNA, followed by second-strand cDNA synthesis. Library quality was verified using an Agilent 2100 Bioanalyzer, and paired-end next-generation sequencing was performed.

7. Statistical Analysis

The two-tailed Student's t-test was used for two-group comparisons. $P < 0.05$ was considered statistically significant. *P*-value annotations were as follows: * denotes $P < 0.05$, ** denotes $P < 0.01$, and *** denotes $P < 0.001$.

Results

1. Screening of Parental Cholangiocarcinoma Cell Lines

CCK-8 assays were performed to detect GEM sensitivity of four CCA cell lines, including three intrahepatic subtypes (HuCCT-1, RBE, HCCC-9810) and one extrahepatic subtype (TFK-1), and corresponding IC_{50} values were calculated. Significant differences in GEM responsiveness were observed among the cell lines (Fig. 1). HuCCT-1 exhibited the highest IC50 (the lowest GEM sensitivity), followed by TFK-1 and HCCC-9810, while RBE was the most susceptible to GEM. These data indicated intrinsic GEM tolerance in HuCCT-1 cells. Therefore, HuCCT-1 and TFK-1 were selected as parental strains for subsequent establishment of resistant sublines and

for subsequent establishment of resistant sublines and molecular characterization.

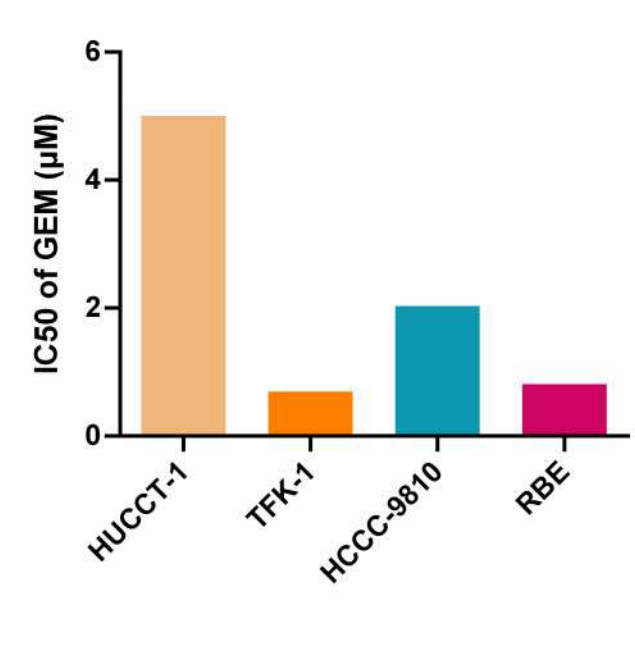


Fig. 1 IC_{50} values of gemcitabine across four cholangiocarcinoma cell lines

2. Establishment and Validation of HuCCT-1-GEM-2 and TFK-1-GEM-2 Resistant Lines

HuCCT-1 cells were subjected to stepwise GEM exposure, starting at 2 μM and increasing by 2 μM per cycle to a final concentration of 40 μM over 18 months. After 2 months of drug-free culture, IC_{50} values were measured. The IC_{50} of HuCCT-1-GEM-2 was 314.5 μM, compared with 12.7 μM in parental HuCCT-1 cells, yielding an RI of 24.8 (Fig. 2).

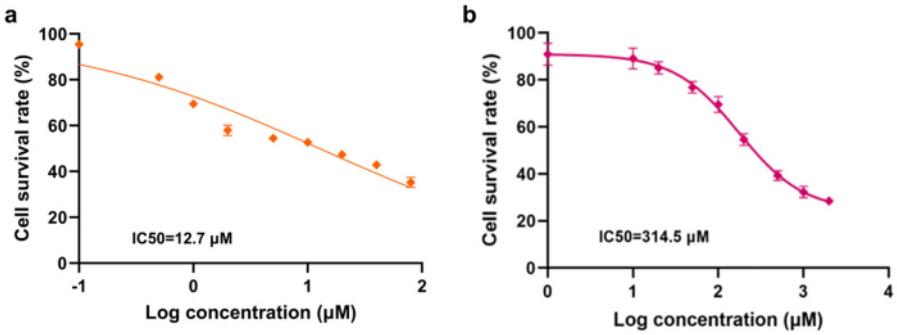


Fig. 2 Gemcitabine IC_{50} curves of HuCCT-1 and HuCCT-1-GEM-2 cells. (a)

Dose-response curve of resistant cells (IC50 = 12.7 μM); (b) Dose-response curve of parental cells (IC50 = 314.5 μM)

For TFK-1 cells, the initial GEM concentration was set at 0.5 μM and was increased by 0.8 μM per cycle to a final concentration of 10 μM over 12 months. After 2 months of drug withdrawal, the IC_{50} of TFK-1-GEM-2 was 9.96 μM, compared with 0.69 μM in the parental TFK-1 cells, yielding an RI of 14.4 (Fig. 3).

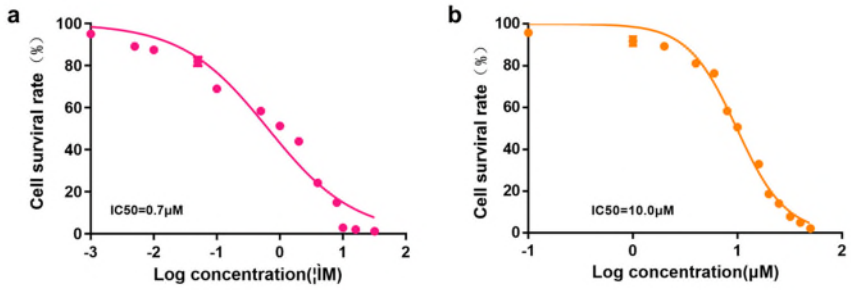


Fig. 3 Gemcitabine IC_{50} curves of TFK-1 and TFK-1-GEM-2 cells. (a) Dose-response curve of TFK-1 (IC50 = 0.7 μM); (b) Dose-response curve of TFK-1-GEM-2 (IC50 = 10.0 μM).Cell survival rates were plotted against log-transformed gemcitabine concentrations

3. Cross-Drug Resistance Profiles of Resistant Cell Lines

CCK-8 assay was used to determine the sensitivity of parental HuCCT-1, resistant HuCCT-1-GEM-2, parental TFK-1, and resistant TFK-1-GEM-2 cells to four chemotherapeutic agents: cisplatin, 5-FU, oxaliplatin, and paclitaxel. Compared with parental cells, HuCCT-1-GEM-2 cells exhibited varying degrees of cross-resistance to several chemotherapeutics; however, no resistance was observed against certain agents (Fig. 4). As shown in Table 2, HuCCT-1-GEM-2 cells displayed prominent cross-resistance to 5-FU and cisplatin, with stronger tolerance to 5-FU, whereas no resistance to oxaliplatin or paclitaxel was detected. In contrast, TFK-1-GEM-2 cells developed cross-resistance to some chemotherapeutic agents but remained sensitive to others. As shown in Fig. 5, TFK-1-GEM-2 cells acquired resistance only to 5-FU, with no significant changes in susceptibility to cisplatin, oxaliplatin, or paclitaxel.

Collectively, the GEM-induced resistant cell lines exhibited selective cross-resistance to other chemotherapeutic agents. The IC_{50} and RI values of all cell lines against each drug are summarized in Tables 2 and 3.

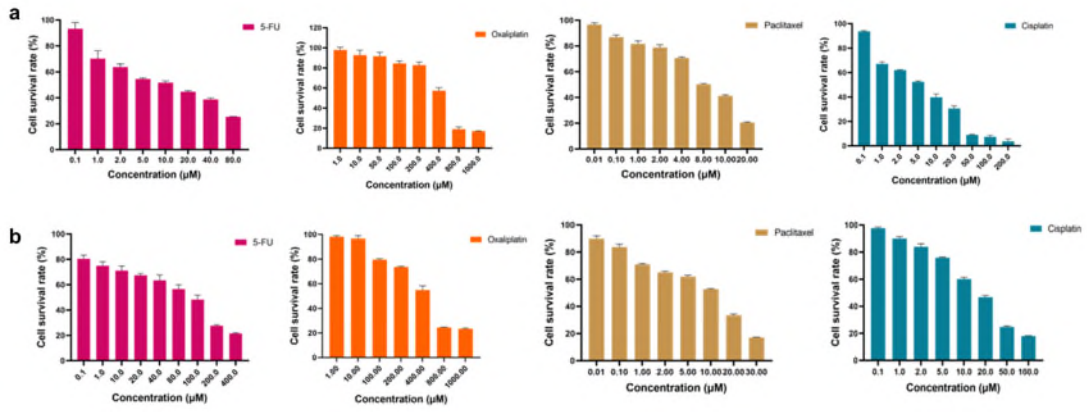


Fig. 4 Drug sensitivity curves of HuCCT-1 and HuCCT-1-GEM-2 for multiple chemotherapeutics. (a) Survival rates of HuCCT-1 treated with gradient concentrations of 5-FU, oxaliplatin, paclitaxel and cisplatin; (b) Survival rates of HuCCT-1-GEM-2 treated with the four chemotherapeutic agents above.

Table 2. IC50 values and RI of HuCCT-1 and HuCCT-1-GEM-2 for various chemotherapeutic agents

Drug	IC50		RI
	HuCCT1（μM）	HuCCT1-GEM-2（μM）	
GEM	12.7	314.5	24.8
5-FU	9.7	64.6	6.7
Oxaliplatin	423.5	400.4	0.9
Paclitaxel	7.5	6.1	0.8
Cisplatin	4.4	16.2	3.7

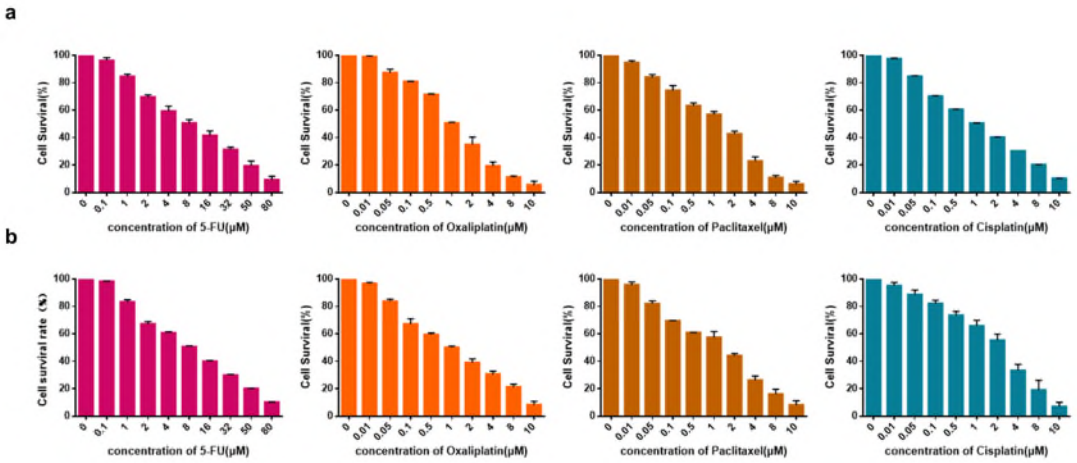


Fig. 5 Drug sensitivity curves of TFK-1 and TFK-1-GEM-2 for multiple chemotherapeutics. (a) Survival rates of TFK-1 treated with gradient concentrations of 5-FU, oxaliplatin, paclitaxel and cisplatin; (b) Survival rates of TFK-1-GEM-2 treated with the four chemotherapeutic agents above.

Table 3. IC_{50} values and RI of TFK-1 and TFK-1-GEM-2 for various chemotherapeutic agents

Drug	IC50		RI
	TFK-1（μM）	TFK-1-GEM-2（μM）	
GEM	0.69	9.96	14.4
5-FU	7.15	31.54	4.4
Oxaliplatin	0.80	0.97	1.2
Paclitaxel	3.78	4.00	1.1
Cisplatin	14.13	15.45	1.1

4. Morphological and Ultrastructural Alterations in Resistant Cells

Under inverted microscopy, both HuCCT-1 and HuCCT-1-GEM-2 exhibited a polygonal adherent morphology. Compared with the parental cells, HuCCT-1-GEM-2 cells displayed an enlarged, irregular cytoplasm, frequent binucleation/multinucleation, and prominent clustered growth (Fig. 6). TEM revealed increased cytoplasmic lipid droplets and vacuoles, along with mitochondrial cristae

rupture and vacuolation in resistant cells (Fig. 7).

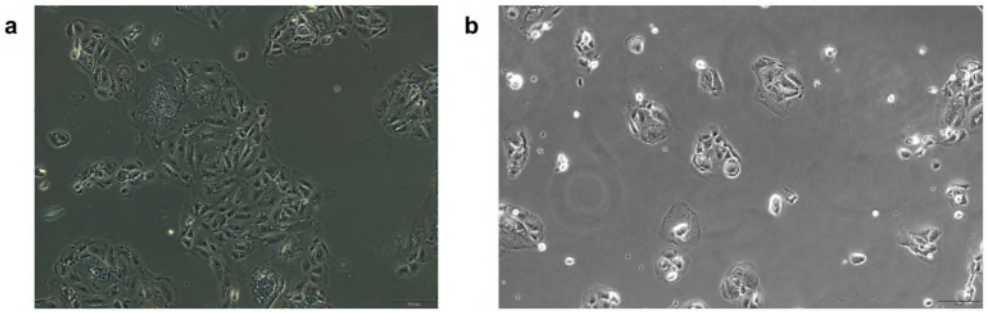


Fig. 6 Inverted microscopy images of HuCCT-1 and HuCCT-1-GEM-2. (a) Parental HuCCT-1 cells; (b) Gemcitabine-resistant HuCCT-1-GEM-2 cells.

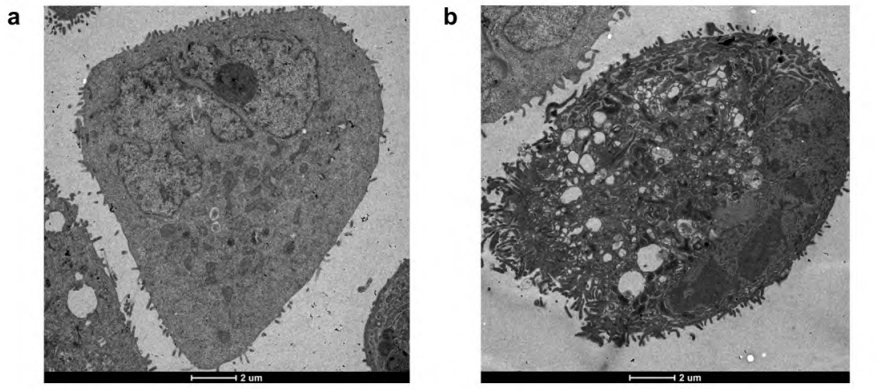


Fig. 7 Transmission electron micrographs of HuCCT-1 and HuCCT-1-GEM-2. (a) Parental HuCCT-1 cell; (b) Gemcitabine-resistant HuCCT-1-GEM-2 cell. Scale bar = 2 μm.

TFK-1 and TFK-1-GEM-2 cells both exhibited a flat, adherent morphology; however, TFK-1-GEM-2 cells were enlarged and irregularly shaped, with abundant intracellular vacuoles and a tendency to form aggregated colonies (Fig. 8). TEM revealed enlarged cells with condensed heterochromatin, disrupted plasma membrane integrity, elevated ribosome abundance, and degenerated mitochondria with disrupted cristae in TFK-1-GEM-2 cells (Fig. 9).

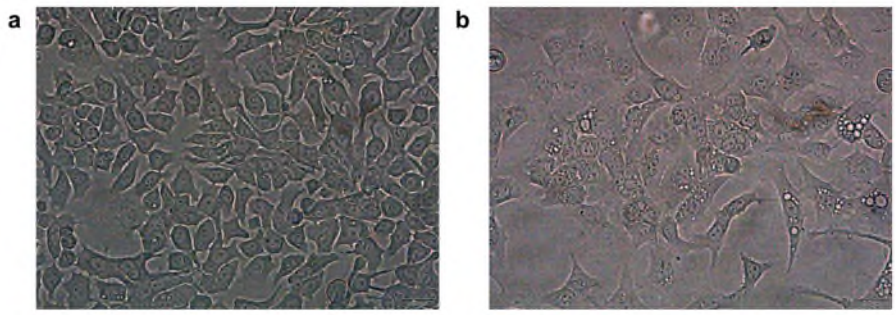


Fig. 8 Inverted microscopy images of TFK-1 and TFK-1-GEM-2. (a) Parental TFK-1 cells; (b) Gemcitabine-resistant TFK-1-GEM-2 cells.

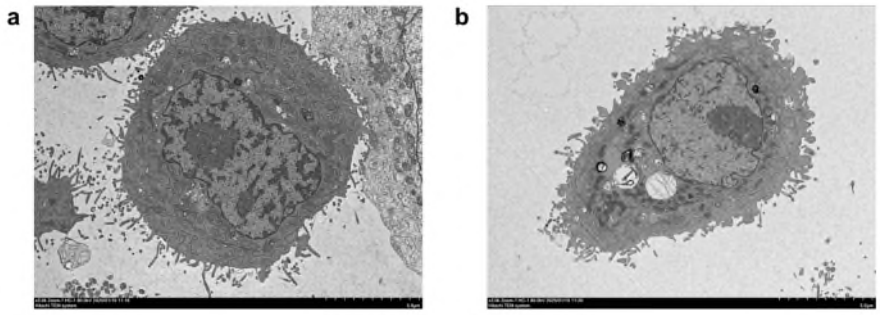


Fig. 9 Transmission electron micrographs of TFK-1 and TFK-1-GEM-2. (a) Parental TFK-1 cell; (b) Gemcitabine-resistant TFK-1-GEM-2 cell. Scale bar = 5 μm.

5. Cell Proliferation Curves

CCK-8 absorbance (OD_{450}) at 0, 24, 48, 72, and 96 h was recorded to evaluate proliferative capacity. The OD values increased in a time-dependent manner in all groups, indicating retained viability in both parental and resistant cells. From 24 h onward, HuCCT-1-GEM-2 cells exhibited significantly lower proliferation than HuCCT-1 cells ($P < 0.05$), with increasing differences over time. Similarly, TFK-1-GEM-2 cells displayed suppressed proliferation from 24 h onward (24 h: **; 48–96 h: ***). These findings indicate that the acquisition of GEM resistance was accompanied by attenuated proliferative activity (Fig. 10).

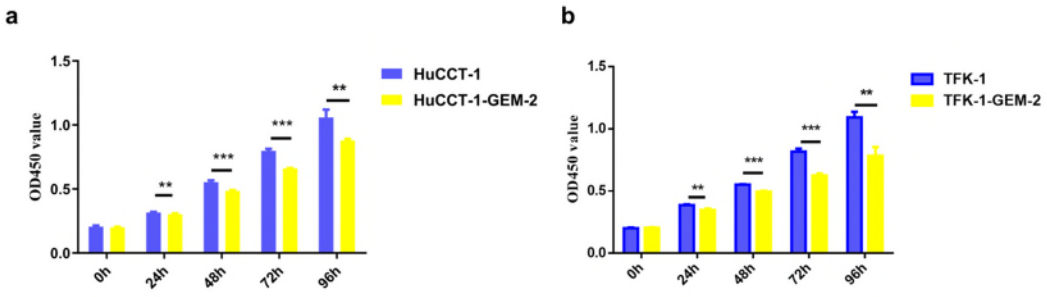


Fig. 10 Proliferation curves. (a) OD_{450} values of HuCCT-1 (blue) and HuCCT-1-GEM-2 (yellow) cells at 0, 24, 48, 72 and 96 h; (b) OD_{450} values of TFK-1 (blue) and TFK-1-GEM-2 (yellow) cells at corresponding time points.

6. Transcriptome Sequencing Analysis

Principal component analysis (PCA) revealed tight clustering of biological replicates and clear separation between parental and resistant cells along PC1, supporting the reliability of the sequencing data and indicating global transcriptional divergence (Fig. 11a and Fig. 12a). Volcano plots identified DEGs using thresholds of $q < 0.05$ and $|\log_2 FC| \geq 1$ (Fig. 11b and Fig. 12b). Hierarchical clustering heatmaps further illustrated the distinct transcriptional signatures between the resistant and parental groups (Fig. 11c and Fig. 12c).

KEGG enrichment of upregulated DEGs in HuCCT-1-GEM-2 cells highlighted NF-κB signaling, cytokine-cytokine receptor interaction, and inflammatory pathways; downregulated genes were enriched in glycolysis/gluconeogenesis, calcium signaling and IL-17 cascades (Fig. 11d-e).

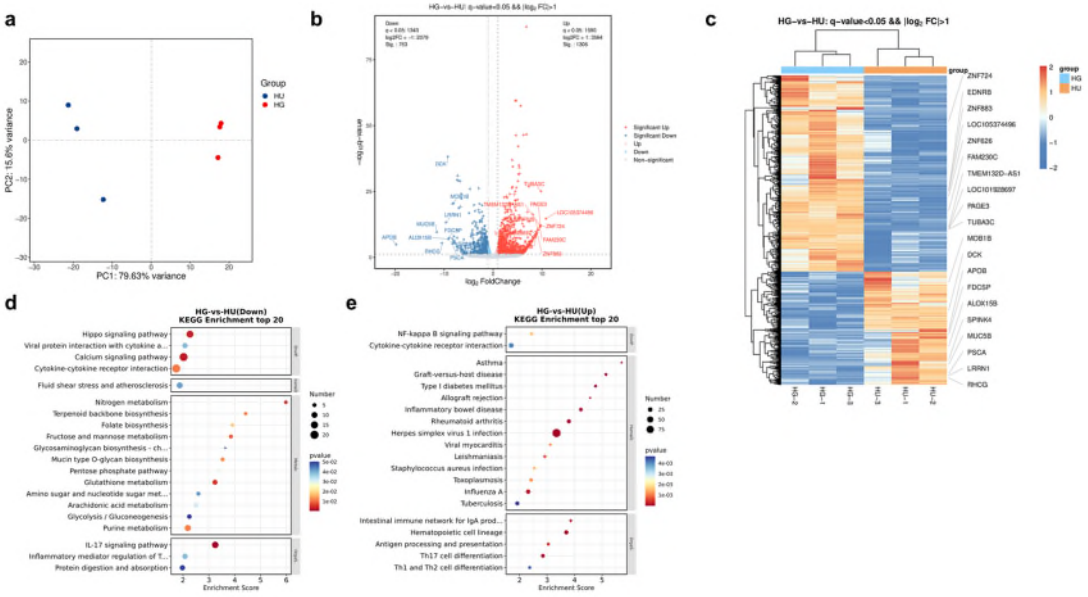


Fig. 11 Transcriptome profiling of HuCCT-1(HU) and HuCCT-1-GEM-2(HG). (a) PCA; (b) Volcano plot; (c) Clustering heatmap; (d) KEGG bubble plot of upregulated DEGs; (e) KEGG bubble plot of downregulated DEGs

In TFK-1-GEM-2 cells, the upregulated DEGs were predominantly enriched in complement and coagulation cascades, sphingolipid metabolism, ECM-receptor interaction, and calcium signaling. Downregulated pathways included TNF, Wnt, and PI3K-Akt signaling (Fig. 12d-e).

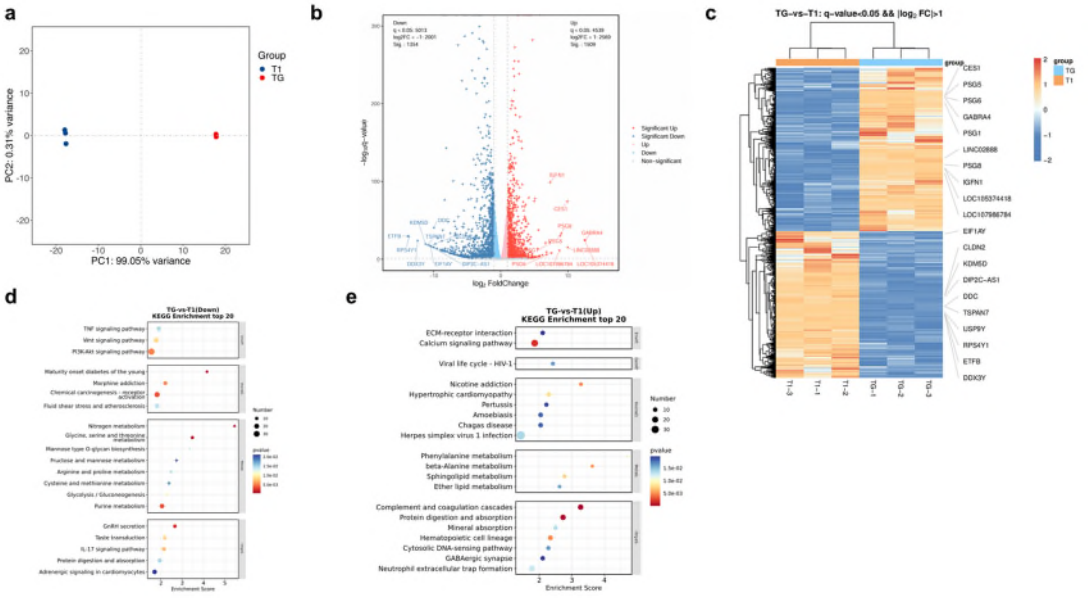


Fig. 12 Transcriptome profiling of TFK-1(T1) and TFK-1-GEM-2(TG). (a) PCA; (b) Volcano

plot; (c) Clustering heatmap; (d) KEGG bubble plot of upregulated DEGs; (e) KEGG bubble plot of downregulated DEGs

7. qRT-PCR Validation of Core Differential Genes

In HuCCT-1-GEM-2 cells, qRT-PCR confirmed a 4.6-fold upregulation of NFKB1 and a 2.3-fold elevation of IL6, reflecting transcriptional activation of NF-κB/inflammatory signaling. The glycolytic genes HK2 and PKM were reduced to 0.8-fold and 0.7-fold, respectively, while IL17A, TNF, and CAV1 were reduced to 0.6-fold, 0.5-fold, and 0.5-fold, respectively, indicating transcriptional suppression of IL-17/TNF pathways.

In TFK-1-GEM-2 cells, the complement gene C3 (showing a 4.0-fold increase) and sphingolipid gene SPHK1 (showing a 2.3-fold increase) were markedly upregulated. HK2, PKM, IL17A, TNF, and CAV1 were all reduced to approximately 0.7-fold, demonstrating shared metabolic and inflammatory remodeling across both resistant subtypes.

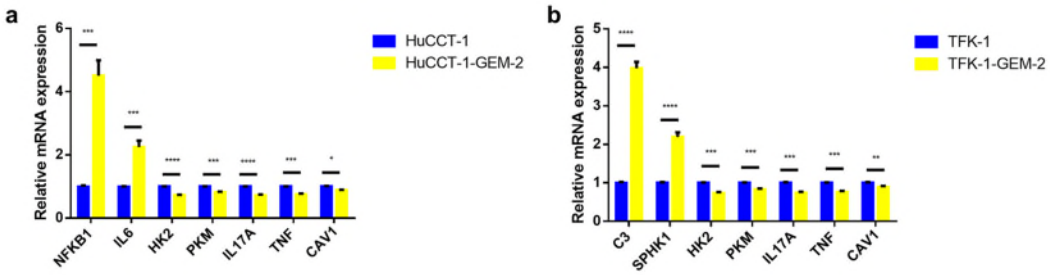


Fig. 13 qRT-PCR detection of inflammation and metabolism-related gene mRNA expression in parental and gemcitabine-resistant cholangiocarcinoma cells. (a) Gene expression comparison between parental HuCCT-1 (blue) and gemcitabine-resistant HuCCT-1-GEM-2 (yellow) cells; (b) Gene expression comparison between parental TFK-1 (blue) and gemcitabine-resistant TFK-1-GEM-2 (yellow) cells.

Discussion

GEM is the core first-line chemotherapeutic agent for advanced CCA, and chemoresistance is the leading cause of clinical treatment failure and poor patient prognosis[12-14]. In this study, two stable GEM-resistant CCA sublines, HuCCT-1-

GEM-2 and TFK-1-GEM-2, were generated after 12–18 months of stepwise drug induction. Drug sensitivity assays confirmed drastically elevated IC_{50} values and high RIs (24.8 and 14.4), verifying stable acquired resistant phenotypes[15]. Cross-resistance experiments revealed selective cross-tolerance to 5-FU in both cell lines, which is consistent with clinical CCA chemoresistance features[16]. These two established cell lines serve as reliable in vitro tools for investigating CCA resistance mechanisms and screening therapeutic targets.

Morphological and ultrastructural remodeling is an adaptive survival response to persistent chemotherapeutic pressure[17, 18]. Resistant cells exhibited an enlarged, aggregated morphology with abundant lipid vacuoles and degenerated mitochondria under TEM[19]. CCK-8 proliferation assays demonstrated suppressed growth kinetics in the resistant strains, indicating that CCA cells suppress proliferation to evade GEM-induced cytotoxicity as a compensatory adaptive strategy[15].

Transcriptome sequencing confirmed robust transcriptional reprogramming in resistant cells, with PCA, volcano, and heatmap analyses verifying clear intergroup transcriptional segregation[20, 21]. KEGG enrichment revealed both shared and cell-specific signaling alterations between intrahepatic- and extrahepatic-resistant CCA. HuCCT-1-GEM-2 shows hyperactivated NF-κB/inflammatory signaling at the transcriptional level, whereas TFK-1-GEM-2 exhibits activated complement and sphingolipid cascades, which are correlated with drug tolerance, with universal suppression of glycolysis and the pro-inflammatory TNF/IL-17 pathways across both subtypes[22-25].

qRT-PCR validated the core transcriptional signatures: NFKB1 and IL6 overexpression is associated with a potential anti-apoptotic resistance phenotype in HuCCT-1-GEM-2, whereas elevated C3 and SPHK1 are correlated with tolerance in TFK-1-GEM-2[26]. Consistently reduced levels of the glycolytic enzymes HK2/PKM and inflammatory mediators indicate universal adaptive metabolic and immune remodeling in GEM-resistant CCA cells[27-29].

Comparative analysis revealed conserved adaptive patterns across the two

models; both resistant lines underwent global metabolic reprogramming with suppressed glycolysis to alleviate oxidative stress and downregulated pro-inflammatory cascades to reduce inflammatory damage, independent of cellular anatomical origin[30-32].

Current studies on CCA GEM resistance have mostly adopted single short-term-induced cell lines, limiting the generalizability of their conclusions[33-36]. This study integrated dual intrahepatic/extrahepatic cell models, phenotypic characterization, ultrastructural observation, and transcriptomic profiling to systematically decode shared and subtype-specific resistance regulatory networks. Our findings advance the current understanding of CCA chemoresistance and identify candidate pathways and genes for combination therapies to overcome drug resistance.

This study has several limitations. First, all the experiments were performed in vitro without in vivo xenograft verification. Second, only transcriptional expression was detected without protein-level validation, gene overexpression/knockdown, or pathway intervention; therefore, the observed associations do not establish causal functions of NFKB1, C3, or SPHK1 in resistance. Third, no clinical tumor cohort was analyzed to correlate these gene signatures with chemotherapy prognosis. In future studies, we aim to establish subcutaneous xenograft models, perform functional verification of candidate genes, and collect clinical specimens to further clarify the molecular mechanisms underlying GEM resistance in CCA.

References

1. EASL Clinical Practice Guidelines on the management of extrahepatic cholangiocarcinoma. J Hepatol. 2025;83(1):211-38. doi:10.1016/j.jhep.2025.03.007.
2. Komuta M. Intrahepatic cholangiocarcinoma: Tumour heterogeneity and its clinical relevance. Clin Mol Hepatol. 2022;28(3):396-407. doi:10.3350/cmh.2021.0287.
3. Cho SY, Hwang H, Kim YH, Yoo BC, Han N, Kong SY et al. Refining Classification of Cholangiocarcinoma Subtypes via Proteogenomic Integration Reveals New Therapeutic Prospects. Gastroenterology. 2023;164(7):1293-309. doi:10.1053/j.gastro.2023.02.045.
4. Ohaegbulam KC, Koethe Y, Fung A, Mayo SC, Grossberg AJ, Chen EY et al. The multidisciplinary management of cholangiocarcinoma. Cancer. 2023;129(2):184-214. doi:10.1002/cncr.34541.
5. Ko S. Trailblazing TRAIL Therapy: Illuminating Pathways for Cholangiocarcinoma Treatment. Cell Mol Gastroenterol Hepatol. 2024;17(5):885-6. doi:10.1016/j.jcmgh.2024.02.008.

6. Bai M, Wang R, Huang C, Zhong R, Jiang N, Fu W et al. Biological and genetic characterization of a newly established human primary multidrug-resistant distal cholangiocarcinoma cell line, CBC3T-6. Sci Rep. 2024;14(1):29661. doi:10.1038/s41598-024-81392-0.
7. Hong JH, Yong CH, Heng HL, Chan JY, Lau MC, Chen J et al. Integrative multiomics enhancer activity profiling identifies therapeutic vulnerabilities in cholangiocarcinoma of different etiologies. Gut. 2024;73(6):966-84. doi:10.1136/gutjnl-2023-330483.
8. Wang J, Liu S, Cao Y, Chen Y. Overcoming treatment resistance in cholangiocarcinoma: current strategies, challenges, and prospects. Front Cell Dev Biol. 2024;12:1408852. doi:10.3389/fcell.2024.1408852.
9. Bai M, Jiang N, Fu W, Huang C, Tian L, Mi N et al. Establishment and characterization of a novel hilar cholangiocarcinoma cell line, CBC3T-1. Hum Cell. 2024;37(1):364-75. doi:10.1007/s13577-023-01003-4.
10. Boyd LNC, Nooijen LE, Ali M, Puik JR, Moustaquim J, Fraga Rodrigues SM et al. Prognostic and predictive value of human equilibrative nucleoside transporter 1 (hENT1) in extrahepatic cholangiocarcinoma: a translational study. Front Pharmacol. 2023;14:1274692. doi:10.3389/fphar.2023.1274692.
11. Lopez-Pascual A, Elurbide J, Valbuena-Goiricelaya E, Latasa MU, Anaya E, Adan-Villaescusa E et al. Transcriptomic profiling of epigenetic regulators and metabolic reprogramming in human cholangiocarcinoma. Front Cell Dev Biol. 2026;14:1765945. doi:10.3389/fcell.2026.1765945.
12. Bridgewater J, Galle PR, Khan SA, Llovet JM, Park JW, Patel T et al. Guidelines for the diagnosis and management of intrahepatic cholangiocarcinoma. J Hepatol. 2014;60(6):1268-89. doi:10.1016/j.jhep.2014.01.021.
13. Cui X, Huang T, Jiang T, Wang H. Current status and prospects of targeted therapy for cholangiocarcinoma based on molecular characteristics. Cancer Lett. 2025;614:217540. doi:10.1016/j.canlet.2025.217540.
14. Yoo C, Hyung J, Chan SL. Recent Advances in Systemic Therapy for Advanced Intrahepatic Cholangiocarcinoma. Liver Cancer. 2024;13(2):119-35. doi:10.1159/000531458.
15. Wattanawongdon W, Hahnvajanawong C, Namwat N, Kanchanawat S, Boonmars T, Jearanaikoon P et al. Establishment and characterization of gemcitabine-resistant human cholangiocarcinoma cell lines with multidrug resistance and enhanced invasiveness. Int J Oncol. 2015;47(1):398-410. doi:10.3892/ijo.2015.3019.
16. Pan YR, Wu CE, Jung SM, Huang SC, Lin SH, Chou WC et al. Mucin 4 Confers Gemcitabine Resistance and an Unfavorable Prognosis in Patients with Cholangiocarcinoma via AKT Activation. Int J Biol Sci. 2023;19(9):2772-86. doi:10.7150/ijbs.79126.
17. Bisht VS, Kumar D, Vats D, Nayak D, Ambatipudi K. Actin-regulated plasticity as a key determinant of the bidirectional switch between chemoresistance and resensitization in triple-positive breast cancer. Life Sci. 2026;393:124321. doi:10.1016/j.lfs.2026.124321.
18. Druzhkova I, Potapov A, Ignatova N, Bugrova M, Shchechkin I, Lukina M et al. Cell hiding in colorectal cancer: correlation with response to chemotherapy in vitro and in vivo. Sci Rep. 2024;14(1):28762. doi:10.1038/s41598-024-79948-1.
19. Thongpon P, Intuyod K, Chomwong S, Pongking T, Klungsaeng S, Muisuk K et al. Curcumin synergistically enhances the efficacy of gemcitabine against gemcitabine-resistant cholangiocarcinoma via the targeting LAT2/glutamine pathway. Sci Rep. 2024;14(1):16059. doi:10.1038/s41598-024-66945-7.

20. Bao X, Li Q, Chen J, Chen D, Ye C, Dai X et al. Molecular Subgroups of Intrahepatic Cholangiocarcinoma Discovered by Single-Cell RNA Sequencing-Assisted Multiomics Analysis. Cancer Immunol Res. 2022;10(7):811-28. doi:10.1158/2326-6066.Cir-21-1101.
21. Tanasuka P, Thongpon P, Chomwong S, Kongsintaweesuk S, Pinlaor S, Pongking T et al. Suppression of kinesin family member-18A diminishes progression and induces apoptotic cell death of gemcitabine-resistant cholangiocarcinoma cells by modulating PI3K/Akt/mTOR and NF-κB pathways. PLoS One. 2025;20(10):e0334147. doi:10.1371/journal.pone.0334147.
22. Liu X, Wang X, Yang Q, Luo L, Liu Z, Ren X et al. Th17 Cells Secrete TWEAK to Trigger Epithelial-Mesenchymal Transition and Promote Colorectal Cancer Liver Metastasis. Cancer Res. 2024;84(8):1352-71. doi:10.1158/0008-5472.Can-23-2123.
23. Propper DJ, Balkwill FR. Harnessing cytokines and chemokines for cancer therapy. Nat Rev Clin Oncol. 2022;19(4):237-53. doi:10.1038/s41571-021-00588-9.
24. Wang Y, Li Y, Zhong J, Li M, Zhou Y, Lin Q et al. Tumor-derived Cav-1 promotes pre-metastatic niche formation and lung metastasis in breast cancer. Theranostics. 2023;13(5):1684-97. doi:10.7150/thno.79250.
25. Dana P, Kariya R, Lert-Itthiporn W, Seubwai W, Saisomboon S, Wongkham C et al. Homophilic Interaction of CD147 Promotes IL-6-Mediated Cholangiocarcinoma Invasion via the NF-κB-Dependent Pathway. Int J Mol Sci. 2021;22(24). doi:10.3390/ijms222413496.
26. Chen MH, Yen CC, Cheng CT, Wu RC, Huang SC, Yu CS et al. Identification of SPHK1 as a therapeutic target and marker of poor prognosis in cholangiocarcinoma. Oncotarget. 2015;6(27):23594-608. doi:10.18632/oncotarget.4335.
27. Cao Y. Adipocyte and lipid metabolism in cancer drug resistance. J Clin Invest. 2019;129(8):3006-17. doi:10.1172/jci127201.
28. Li M, Yang Y, Xiong L, Jiang P, Wang J, Li C. Metabolism, metabolites, and macrophages in cancer. J Hematol Oncol. 2023;16(1):80. doi:10.1186/s13045-023-01478-6.
29. Tan Y, Li J, Zhao G, Huang KC, Cardenas H, Wang Y et al. Metabolic reprogramming from glycolysis to fatty acid uptake and beta-oxidation in platinum-resistant cancer cells. Nat Commun. 2022;13(1):4554. doi:10.1038/s41467-022-32101-w.
30. Adrover JM, Han X, Sun L, Fujii T, Sivetz N, Daßler-Plenker J et al. Neutrophils drive vascular occlusion, tumour necrosis and metastasis. Nature. 2025;645(8080):484-95. doi:10.1038/s41586-025-09278-3.
31. Geng L, Yang X, Sun J, Ran X, Zhou D, Ye M et al. Gut Microbiota Modulation by Inulin Improves Metabolism and Ovarian Function in Polycystic Ovary Syndrome. Adv Sci (Weinh). 2025;12(20):e2412558. doi:10.1002/advs.202412558.
32. Hidalgo-García L, Ruiz-Malagon AJ, Huertas F, Rodríguez-Sojo MJ, Molina-Tijeras JA, Diez-Echave P et al. Administration of intestinal mesenchymal stromal cells reduces colitis-associated cancer in C57BL/6J mice modulating the immune response and gut dysbiosis. Pharmacol Res. 2023;195:106891. doi:10.1016/j.phrs.2023.106891.
33. Zhen Y, Liu K, Shi L, Shah S, Xu Q, Ellis H et al. FGFR inhibition blocks NF-κB-dependent glucose metabolism and confers metabolic vulnerabilities in cholangiocarcinoma. Nat Commun. 2024;15(1):3805. doi:10.1038/s41467-024-47514-y.
34. Jiang K, Yang W, Huang J, Tan X, Liu Y, Tu S et al. SENP1 promotes p27kip1 nuclear export though enhanced SUMOylation in cholangiocarcinoma leading to increased cell proliferation and chemoresistance. Int J Mol Med. 2025;56(3). doi:10.3892/ijmm.2025.5582.

35. Li X, Song Z, Lin S, Luo M, Liu S, Liu Y et al. The allosteric IDH1 inhibitor ivosidenib overcomes chemoresistance in intrahepatic cholangiocarcinoma models expressing wild-type IDH1. J Clin Invest. 2026;136(10). doi:10.1172/jci199730.
36. Puthdee N, Khramchantuk S, Nuwongsri P. LIN28B Enhanced STAT3 Signaling Regulates Inflammatory Response and Chemotherapeutic Resistance in Cholangiocytes. Asian Pac J Cancer Prev. 2021;22(11):3671-8. doi:10.31557/apjcp.2021.22.11.3671.

Declarations

Funding

National Natural Science Foundation of China (NSFC), 82560492

National Natural Science Foundation of China (NSFC), 82460568

Gansu Provincial Department of Science and Technology, 23JRRA1488

Conflict of interest

The authors declare no conflicts of interest.

Ethical approval

Not applicable.

Informed consent

Not applicable.